

## Metal-Substituted Disilynes with Linear Forms

Masae Takahashi\* and Yoshiyuki Kawazoe

Institute for Materials Research, Tohoku University, Sendai 980-8577, Japan

Received May 23, 2008

**Summary:** The present systematic survey of linear disilynes  $\text{ESi}\equiv\text{SiE}$  with various metal elements  $E$  by *ab initio* and density functional theory calculations has shown that magnesium is highly suited to stabilize the linear conformation of the  $\text{Si}\equiv\text{Si}$  bond. A synthetically accessible model compound using the magnesium complex of a core-modified porphyrin as a substituent has been designed.

A triple bond is classically seen to have a linear structure with a very short bond distance, as found in acetylene ( $\text{HC}\equiv\text{CH}$ ). A symmetry-separated set of one  $\sigma$  and two degenerate  $\pi$  molecular orbitals describes the set of six valence electrons in a triple bond in the common molecular orbital theory using delocalized orbitals. Though the electronic structure of silicon is analogous to that of carbon, according to the multiple-bond rule silicon is not capable of forming multiple bonds because of the considerable Pauli repulsion between the electrons of inner shells.<sup>1–3</sup> Submillimeter-wave rotational spectroscopic studies of a low-power silane plasma by Bogey and co-workers have revealed the structures of the doubly hydrogen bonded  $\text{H}_2\text{Si}_2$  (**1**;  $C_{2v}$  symmetry) with a Si–Si bond length of 2.208 Å and the singly bridged  $\text{H}_2\text{Si}_2$  (**2**;  $C_s$  symmetry) with a very short Si–Si separation of 2.119 Å (Figure 1).<sup>4,5</sup> The experiment verified an earlier theoretical prediction by Lischka and Köhler<sup>6</sup> of the doubly hydrogen bonded structure as the global minimum of the  $\text{H}_2\text{Si}_2$  singlet potential surface. The monobridged structure is the second most stable isomer of  $\text{H}_2\text{Si}_2$ .<sup>7,8</sup> The acetylene analogue **3** with  $D_{\infty h}$  symmetry does not even correspond to a minimum on the potential surface and distorts to the  $C_{2h}$ -symmetrical trans-bent form **4**.<sup>9</sup> The bending is accompanied by a loss of  $\pi$ -bond strength and a lowering of the bond order.<sup>10,11</sup> Until recently the isolation of a stable molecule with a Si–Si triple bond (disilyne) remained a challenge. Sekiguchi and co-workers have achieved the first isolation and characterization of a stable disilyne (1,1,4,4-tetrakis[bis(trimethylsilyl)methyl]-1,4-diisopropyl-2-tetrasylyne) with a formal Si–Si triple bond.<sup>12</sup> The solid-state structure of the disilyne was confirmed by X-ray crystallographic analysis to be trans-bent with a bond angle of 137.44°, and the four Si atoms are perfectly coplanar. The Si–Si triple-bond length

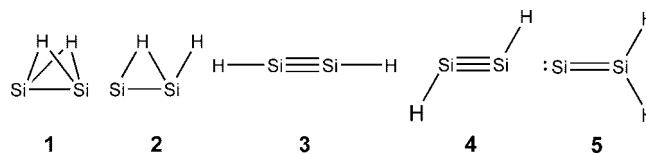


**Figure 1.**  $\text{Si}_2\text{H}_2$  isomers: **1**, dibridged; **2**, monobridged; **3**, linear; **4**, trans-bent; **5**, disilavinylidene.

of 2.062 Å is 3.8% shorter than the typical double-bond length (2.14 Å) and 13.5% shorter than the average single-bond length (2.34 Å). The structure is close to that of  $(\text{tBu}_3\text{Si})_2\text{MeSiSi}\equiv\text{SiSiMe}(\text{tBu}_3\text{Si})_2$  calculated by density functional theory (DFT), where tBu is *tert*-butyl.<sup>13</sup> Along with the report by West<sup>14</sup> the synthesis of the stable disilyne by Sekiguchi and co-workers is a milestone both for silicon chemistry and for multiple-bond chemistry in general. Returning to the multiple-bond rule, however, the difficulty in forming a classical linear Si–Si triple bond has not been conquered. Though a natural bond order analysis of the disilyne by Sekiguchi et al. gives a value of 2.618, indicating a nearly genuine triple bond, compared with about 2 in the formal digermene<sup>15,16</sup> and distannene<sup>15,17</sup> and only 1 in the formal diplumbyne,<sup>15,18</sup> the value is still less than that of 3 for acetylene. The isolated disilyne is not linear but trans-bent, and in addition the use of a sterically overcrowded substituent gives it kinetic instability. It has been shown theoretically that substitution by electropositive silyl groups is electronically much more effective in realizing a less trans-bent disilyne structure.<sup>19,20</sup> However, neither theoretical nor experimental attempts have succeeded in obtaining a linear  $D_{\infty h}$ -symmetrical geometry as the global minimum.

We have been investigating theoretically the stability<sup>21–23</sup> and reactivity<sup>24,25</sup> of unsaturated silicon compounds. In this paper, we report the systematic search for stable linear disilynes  $\text{ESi}\equiv\text{SiE}$  by *ab initio* and DFT calculations. Since disilyne with an electropositive silyl group has a less trans-bent structure,<sup>19,20</sup> we utilize metal elements ( $E = \text{Li, Na, K, Be, Mg, Ca, Sc, Ti, V, Cr, Mn, Fe, Co, Ni, Cu, Zn}$ ) as much more electropositive substituents. Recently, we have found that charged systems are helpful for understanding systematically the stability of the silicon  $\pi$  system<sup>22</sup> and more recently designed an aromatic silicon six-membered ring with  $D_{6h}$  symmetry using a negatively charged system.<sup>23</sup> Numerous investigations on the substituent effects of disilynes have been performed so far, but this is the first attempt to use metal substituents, to the best of our knowledge.

(13) Takagi, N.; Nagase, S. *Eur. J. Inorg. Chem.* **2002**, 2775.

(14) West, R. *Science* **2004**, 305, 1724.

(15) Weidenbruch, M. *Angew. Chem., Int. Ed.* **2005**, 44, 514.

(16) Stender, M.; Phillips, A. D.; Wright, R. J.; Power, P. P. *Angew. Chem., Int. Ed.* **2002**, 41, 1785.

(17) Phillips, A. D.; Wright, R. J.; Olmstead, M. M.; Power, P. P. *J. Am. Chem. Soc.* **2002**, 124, 5930.

(18) Pu, L.; Twamley, B.; Power, P. P. *J. Am. Chem. Soc.* **2000**, 122, 3524.

(19) Kobayashi, K.; Nagase, S. *Organometallics* **1997**, 16, 2489.

(20) Nagase, S.; Kobayashi, K.; Takagi, N. *J. Organomet. Chem.* **2000**, 611, 264.

\*To whom correspondence should be addressed. E-mail: masae@imr.edu.

(1) Wiberg, E. In *Lehrbuch der Anorganischen Chemie*; Holleman, A. F., Wiberg, E., Eds.; de Gruyter: Berlin, 1943; Vols. 22 and 23.

(2) Goubeau, J. *Angew. Chem.* **1957**, 69, 77.

(3) Jutzi, P. *Angew. Chem., Int. Ed. Engl.* **1975**, 14, 232.

(4) Bogey, M.; Bolvin, H.; Demuyne, C.; Destombes, J.-L. *Phys. Rev. Lett.* **1991**, 66, 413.

(5) Cordonnier, M.; Bogey, M.; Demuyne, C.; Destombes, J.-L. *J. Chem. Phys.* **1992**, 97, 7984.

(6) Lischka, H.; Köhler, H.-J. *J. Am. Chem. Soc.* **1983**, 105, 6646.

(7) Colegrove, B. T.; Schaefer, J. F., III *J. Phys. Chem.* **1990**, 94, 5593.

(8) Grev, R. S.; Schaefer, H. F., III *J. Chem. Phys.* **1992**, 97, 7990.

(9) For a review, see: Grev, R. S. *Adv. Organomet. Chem.* **1991**, 33, 125.

(10) Bridgeman, A. J.; Ireland, L. R. *Polyhedron* **2001**, 20, 2841.

(11) Grunenberg, J. *Angew. Chem., Int. Ed.* **2001**, 40, 4027.

(12) Sekiguchi, A.; Kinjo, R.; Ichinohe, M. *Science* **2004**, 305, 1755.

**Table 1. Characteristics of Stationary Points, Wiberg Bond Indices (BO), Silicon–Silicon Bond Lengths ( $r_{\text{SiSi}}$ ), and Natural Population Analysis Charges at Si ( $q_{\text{Si}}$ ) of Linear  $\text{ESi}\equiv\text{SiE}^a$** 

E	MP2				B3LYP			
	stationary point	BO	$r_{\text{SiSi}}$ (Å)	$q_{\text{Si}}$ (e)	stationary point	BO	$r_{\text{SiSi}}$ (Å)	$q_{\text{Si}}$ (e)
Li	TS(2)	3.041	2.111	−0.898	TS(2)	2.992	2.079	−0.853
Na	TS(2)	3.034	2.113	−0.891	TS(2)	2.980	2.077	−0.788
K	TS(2)	3.031	2.125	−0.941	TS(2)	2.965	2.094	−0.840
Be	MIN	2.866	2.102	−0.645	TS(2)	2.822	2.077	−0.585
Mg	MIN	2.923	2.119	−0.647	TS(2)	2.912	2.081	−0.592
Ca	MIN	2.951	2.156	−0.836	TS(2)	2.863	2.089	−0.727
Sc	MIN	1.100	2.259	−1.121	MIN	1.926	2.174	−0.599
Ti	ND				MIN	1.162	2.307	−0.272
V	MIN	1.037	2.285	−0.618	MIN	1.154	2.299	−0.010
Cr	ND				MIN	1.138	2.302	0.025
Mn	ND				MIN	1.128	2.314	0.015
Fe	MIN	1.924	2.257	−0.634	TS(1)	1.960	2.160	−0.203
Co	ND				MIN	1.100	2.334	0.058
Ni	TS(2)	1.958	2.300	−0.353	TS(1)	1.897	2.183	−0.113
Cu	TS(2)	3.001	2.063	−0.731	TS(2)	2.929	2.033	−0.529
Zn	MIN	2.902	2.123	−0.546	TS(2)	2.921	2.082	−0.447
HC≡CH	MIN	2.993	1.210	−0.220	MIN	2.996	1.196	−0.222

<sup>a</sup> Optimized at the MP2 and B3LYP levels using the 6-311+G(3df) basis set. Legend: TS(2), second-order saddle point; TS(1), first-order saddle point, which corresponds to a transition state linking two minima; MIN, minimum; ND, not optimized.

Calculations were performed with the use of the Gaussian 03 software package.<sup>26</sup> We basically utilized the 6-311+G(3df) basis set,<sup>27</sup> but for the calculation of large molecules the level of the basis set was lowered. To display MP2 orbitals, natural orbitals were generated by diagonalizing one particle density matrix. In the DFT calculations, we used the hybrid Becke-type three-parameter exchange functional<sup>28</sup> paired with the gradient-corrected Lee, Yang, and Parr correlation functional

(B3LYP),<sup>29,30</sup> as well as with the gradient-corrected Perdew–Wang 91 correlation functional (B3PW91).<sup>31,32</sup> An important feature of the density-functional method is the fact that it takes into account many-electron correlations via the phenomenological exchange-correlation potential. However, so far, a unique potential has not been found to be universally applicable for different systems and conditions. As a result, there are many different parametrizations for the exchange-correlation potential valid for special cases. A direct ab initio method based on the consistent post-Hartree–Fock many-body theory is the alternative. In the present work, we applied the Møller–Plesset perturbation theory of the second (MP2) and the fourth (MP4) orders.<sup>33</sup> Since the fundamental physical principles are free from any phenomenological parameters, this model can be refined by extending the quality of the approximations, while the physical meaning of the effects included is clearly demonstrated. Thus, often such an approach predicts characteristics more accurately and reliably than the DFT.

(21) (a) Veszprémi, T.; Takahashi, M.; Hajgató, B.; Ogasawara, J.; Sakamoto, K.; Kira, M. *J. Phys. Chem. A* **1998**, *102*, 10530. (b) Takahashi, M.; Tsutsui, S.; Sakamoto, K.; Kira, M.; Müller, T.; Apeloig, Y. *J. Am. Chem. Soc.* **2001**, *123*, 347. (c) Takahashi, M.; Kira, M.; Sakamoto, K.; Müller, T.; Apeloig, Y. *J. Comput. Chem.* **2001**, *22*, 1536. (d) Takahashi, M.; Sakamoto, K. *J. Phys. Chem. A* **2004**, *108*, 5710.

(22) (a) Takahashi, M.; Sakamoto, K. *Organometallics* **2002**, *21*, 4212. (b) Takahashi, M.; Sakamoto, K. *Phosphorus, Sulfur Silicon Relat. Elem.* **2002**, *177*, 1721.

(23) (a) Takahashi, M.; Kawazoe, Y. *Organometallics* **2005**, *24*, 2433. (b) Takahashi, M.; Kawazoe, Y. *Chem. Phys. Lett.* **2006**, *418*, 475. (c) Takahashi, M.; Kawazoe, Y. *Comput. Mater. Sci.* **2006**, *36*, 30.

(24) Thermal reactions: (a) Veszprémi, T.; Takahashi, M.; Ogasawara, J.; Sakamoto, K.; Kira, M. *J. Am. Chem. Soc.* **1998**, *120*, 2408. (b) Takahashi, M.; Veszprémi, T.; Hajgató, B.; Kira, M. *Organometallics* **2000**, *19*, 4660. (c) Veszprémi, T.; Takahashi, M.; Hajgató, B.; Kira, M. *J. Am. Chem. Soc.* **2001**, *123*, 6629. (d) Takahashi, M.; Veszprémi, T.; Sakamoto, K.; Kira, M. *Mol. Phys.* **2002**, *100*, 1703. (e) Hajgató, B.; Takahashi, M.; Kira, M.; Veszprémi, T. *Chem. Eur. J.* **2002**, *8*, 2126. (f) Takahashi, M.; Veszprémi, T.; Kira, M. *Organometallics* **2004**, *23*, 5768.

(25) Photochemical reactions: (a) Takahashi, M.; Sakamoto, K. *J. Phys. Chem. A* **2004**, *108*, 7301. (b) Takahashi, M. *J. Phys. Chem. A* **2005**, *109*, 11902.

(26) Frisch, M. J.; Trucks, G. W.; Schlegel, H. B.; Scuseria, G. E.; Robb, M. A.; Cheeseman, J. R.; Montgomery, J. A., Jr.; Vreven, T.; Kudin, K. N.; Burant, J. C.; Millam, J. M.; Iyengar, S. S.; Tomasi, J.; Barone, V.; Mennucci, B.; Cossi, M.; Scalmani, G.; Rega, N.; Petersson, G. A.; Nakatsuji, H.; Hada, M.; Ehara, M.; Toyota, K.; Fukuda, R.; Hasegawa, J.; Ishida, M.; Nakajima, T.; Honda, Y.; Kitao, O.; Nakai, H.; Klene, M.; Li, X.; Knox, J. E.; Hratchian, H. P.; Cross, J. B.; Bakken, V.; Adamo, C.; Jaramillo, J.; Gomperts, R.; Stratmann, R. E.; Yazyev, O.; Austin, A. J.; Cammi, R.; Pomelli, C.; Ochterski, J. W.; Ayala, P. Y.; Morokuma, K.; Voth, G. A.; Salvador, P.; Dannenberg, J. J.; Zakrzewski, V. G.; Dapprich, S.; Daniels, A. D.; Strain, M. C.; Farkas, O.; Malick, D. K.; Rabuck, A. D.; Raghavachari, K.; Foresman, J. B.; Ortiz, J. V.; Cui, Q.; Baboul, A. G.; Clifford, S.; Cioslowski, J.; Stefanov, B. B.; Liu, G.; Liashenko, A.; Piskorz, P.; Komaromi, I.; Martin, R. L.; Fox, D. J.; Keith, T.; Al-Laham, M. A.; Peng, C. Y.; Nanayakkara, A.; Challacombe, M.; Gill, P. M. W.; Johnson, B.; Chen, W.; Wong, M. W.; Gonzalez, C.; Pople, J. A. *Gaussian 03, Revision C.02-E.01*; Gaussian, Inc., Wallingford, CT, 2004.

(27) Foresman, J. B.; Frisch, A. In *Exploring Chemistry with Electronic Structure Methods*; Gaussian Inc., Pittsburgh, PA, 1996.

(28) Becke, A. D. *J. Chem. Phys.* **1993**, *98*, 5648.

Geometries of singlet  $\text{ESi}\equiv\text{SiE}$  ( $\text{E} = \text{Li, Na, K, Be, Mg, Ca, Sc, Ti, V, Cr, Mn, Fe, Co, Ni, Cu, Zn}$ ) were optimized under  $D_{\infty h}$ -symmetrical constraint. B3LYP and B3PW91 gave similar results, and thus only the result of B3LYP is shown in Table 1. Optimized silicon–silicon bond distances are shorter at the B3LYP level than at the MP2 level, except for  $\text{VSi}\equiv\text{SiV}$ . Natural population analysis (NPA) charges at silicon are less negative at the B3LYP level than at the MP2 level. The most substantial difference between the MP2 and B3LYP levels is the nature of stationary points (a minimum or a saddle point). Minimum characters are obtained for  $\text{E} = \text{Be, Mg, Ca, Sc, V, Fe, Zn}$  at the MP2 level and for  $\text{E} = \text{Sc, Ti, V, Cr, Mn, Co}$  at the B3LYP level. The Wiberg bond index<sup>34</sup> is around 3 for  $\text{E} = \text{Li, Na, K, Be, Mg, Ca, Cu, Zn}$ , indicating a triple bond. Those have short silicon–silicon distances (2.06–2.16 Å at the MP2 level and 2.03–2.09 Å at the B3LYP level) compared with the others (2.26–2.30 Å at the MP2 level and 2.16–2.33 Å at the B3LYP level). Their NPA charge at silicon is negative (−0.941 to −0.546 at the MP2 level and −0.853 to −0.447 at the B3LYP

(29) Lee, C.; Yang, W.; Parr, R. G. *Phys. Rev. B* **1988**, *37*, 785.

(30) Vosko, S. H.; Wilk, L.; Nusair, M. *Can. J. Phys.* **1980**, *58*, 1200.

(31) Perdew, J. P. In *Electronic Structure of Solids '91*; Ziesche, P., Eschrg, H., Eds.; Academic Verlag: Berlin, 1991; p 11.

(32) Burke, K.; Perdew, J. P.; Yang, Y. In *Electronic Density Functional Theory: Recent Progress and New Directions*; Dobson, J. F., Vignale, G., Das, M. P., Eds.; Plenum: New York, 1998.

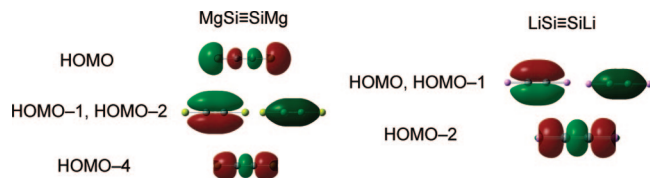


**Figure 2.** Molecular orbitals of  $\text{MgSi}\equiv\text{SiMg}$  and  $\text{LiSi}\equiv\text{SiLi}$  using the generalized density for MP2 at the MP2/6-311+G(3df) geometry.

level) for  $E = \text{Li, Na, K, Be, Mg, Ca, Cu, Zn}$ , indicating that the metals act as electron donors.

A classical triple-bond structure, i.e. a linear form with a Wiberg bond index of approximately 3, is obtained as a minimum only for divalent-metal-substituted disilynes ( $\text{ESi}\equiv\text{SiE}$ ;  $E = \text{Be, Mg, Ca, Zn}$ ), where the atomic electron configuration of the metals is  $s^2$ . In addition, the linear forms are minima only by the MP2 method and are saddle points by the B3LYP method. This would be due to the fact that, in the study of binding with a closed electronic subshell element such as a divalent metal, the contribution of an attractive dispersion force is important and is not correctly treated by the DFT method. Although the monovalent-metal-substituted disilynes ( $\text{ESi}\equiv\text{SiE}$ ;  $E = \text{Li, Na, K, Cu}$ ) have a Wiberg bond index of approximately 3 in the linear form where the atomic electron configuration of the metals is  $s$ , those are second-order saddle points by both the MP2 and B3LYP methods. Six valence electrons are accommodated in one  $\sigma$  and two degenerate  $\pi$  molecular orbitals in both divalent- and monovalent-metal-substituted disilynes, as in the case of the classical triple bond (Figure 2). The realization of the classical triple bond only in divalent-metal-substituted disilynes is explained by the suppression of  $\sigma-\pi$  mixing. A donor-acceptor bonding model has well explained the trans-bent structure of disilyne ( $\text{HSi}\equiv\text{SiH}$ ), where a triple bond weakened by distortion from a classical linear structure is stabilized by the delocalization of the  $n_s$  lone electron pair of one SiH into the empty  $p_{\pi}^*$  atomic orbital of its partner in the valence bond scheme. Explaining the donor-acceptor bonding model in the molecular orbital scheme, the distorted structure is stabilized by  $\sigma-\pi$  mixing. The  $\sigma-\pi$  mixing would be suppressed in the divalent-metal-substituted disilynes by the highest occupied molecular orbital (HOMO), which is neither a  $\sigma$  nor a  $\pi$  orbital. The HOMO's of the divalent-metal-substituted disilynes have the same shape and are neither  $\sigma$  nor  $\pi$  orbitals (the HOMO of  $\text{MgSi}\equiv\text{SiMg}$  is shown in Figure 2). The remarkable difference of the linear monovalent substituents in comparison to the linear divalent substituents in their molecular orbitals is that the HOMO of the monovalent-metal-substituted disilynes is a  $\pi$  orbital (the HOMO of  $\text{LiSi}\equiv\text{SiLi}$  is shown in Figure 2).

Isomers of the divalent-metal-substituted disilynes on ground-state potential surfaces were searched for at the MP2/6-311+G(3df) level. For  $\text{H}_2\text{Si}_2$ , four isomers of dibridged **1**, monobridged **2**, trans-bent **4**, and disilavinylidene **5** are known. The global minimum is **1** followed by **2**, **5**, and **4**.<sup>7,8,23a</sup> Linear structure **3** is not a minimum on the potential surface of  $\text{H}_2\text{Si}_2$ . Starting from the four conformations (**1**, **2**, **4**, and **5**), we finally obtained two isomers for  $\text{Be}_2\text{Si}_2$  (**1**, **2**) and  $\text{Zn}_2\text{Si}_2$  (**1**, **5**) and one isomer for  $\text{Mg}_2\text{Si}_2$  (**5**) and  $\text{Ca}_2\text{Si}_2$  (**1**). The optimized structures and relative energies are shown in Figure 3. It is notable that no trans-bent form **4** is obtained as a minimum. The linear form is not the most stable isomer in  $\text{Be}_2\text{Si}_2$  and  $\text{Zn}_2\text{Si}_2$ , while that form is more stable than the other isomer in  $\text{Mg}_2\text{Si}_2$  and  $\text{Ca}_2\text{Si}_2$ . The relative stability difference between the  $\text{Ca}_2\text{Si}_2$  isomers is very small (0.28 kcal/mol), and thus two isomers would coexist. On the other hand, the relative stability difference between the  $\text{Mg}_2\text{Si}_2$  isomers is large enough (12.84

kcal/mol) to give a linear disilyne without any kinetic stabilization against isomerization. The relative stability among isomers is qualitatively explained by the molecular orbitals (Figure 3). The HOMO of the disilavinylidene isomer in  $\text{Mg}_2\text{Si}_2$  and  $\text{Zn}_2\text{Si}_2$  consists of  $\pi_{\text{SiSi}}$  and metal 3s in an antibonding manner by the repulsive interaction between the occupied orbitals, leading to the destabilization of the disilavinylidene isomer. The orbital consisting of  $\pi_{\text{SiSi}}$  and 3s in an antibonding manner is the lowest unoccupied molecular orbital (LUMO) in the dibridged  $\text{Zn}_2\text{Si}_2$  and  $\text{Be}_2\text{Si}_2$  isomers, leading to stabilization. In the monobridged  $\text{Be}_2\text{Si}_2$  and the dibridged  $\text{Ca}_2\text{Si}_2$  isomers, the HOMO's consist of  $\pi_{\text{SiSi}}$  and metal p or d orbitals in a bonding manner.

To confirm the preference of a linear structure in  $\text{Mg}_2\text{Si}_2$ , we refined the calculation by extending the quality of the approximation up to MP4. Both the linear and disilavinylidene forms are obtained as minima at the MP4(SDTQ)/6-311+G(3df) level, and the linear form is more stable by 12.06 kcal/mol with a zero-point vibration energy (ZPVE) correction. To elucidate the bonding nature of the linear  $\text{MgSi}\equiv\text{SiMg}$ , a natural bond orbital (NBO) analysis<sup>35</sup> was performed at the MP2/6-311+G(3df) level, where the occupancy threshold for the NBO search was taken to be 1.60. There are 26 occupied orbitals: 20 core, 3 bonding, 1 nonbonding, and 2 lone pair. The hybridizations are two  $p_{\pi}$  (99.57%) at Si of bonding Si-Si and one  $sp^{3.33}$  at Si of bonding Si-Si, one  $s$  type (99.86%) at Mg of nonbonding Mg-Mg, and an  $s$ -type (77.08%) lone pair at each Si atom. The hybridizations at Si can be explained by the Zintl-Klemm electron counting concept.<sup>36</sup> The basic idea behind the Zintl-Klemm concept is the transfer of electrons from more electropositive elements to more electronegative elements, with the potential for the formation of strong bonds between the latter. This protocol usually works well with alkali-metal, alkaline-earth-metal, and rare-earth elements as electron donors. Conforming to the Zintl-Klemm electron counting concept, upon completing the octet, Si in a triple-bond pair should be  $-2$ , and thus the bonding is described as  $\text{Mg}^+[\text{Si}\equiv\text{Si}]^{2-}\text{Mg}^+$ , where an  $\text{Si}_2$  pair contains two  $\pi$ , one  $\sigma$ , and two lone-pair orbitals as obtained by the NBO analysis. As shown in Table 1, the NPA charge of  $\text{MgSi}\equiv\text{SiMg}$  at silicon is strongly negative ( $-0.647$ ), suggesting electron transfer from Mg.  $\text{Mg}^+$  is realized by a doubly occupied nonbonding orbital in the closed-shell system. In this sense, it may be of interest to investigate the open-shell system such as singlet biradical and/or triplet species. Instability with respect to relaxation of the constraint to the RHF wave function for single-determinant wave functions was actually found, but the singlet state of linear  $\text{MgSi}\equiv\text{SiMg}$  is more stable by 0.93 kcal/mol than the triplet state at the UB3LYP/6-311+G(3df) level with a ZPVE correction.

It is found in the present calculations that a Mg-substituted disilyne is the best candidate to obtain a linear conformation. To render the linear disilyne synthetically more accessible, we designed the Mg-substituted disilyne using the magnesium complex of core-modified porphyrin. Core-modified porphyrins resulting from the replacement of one or two pyrrole rings by heterocycles are frequently used to stabilize metals in uncommon oxidation states.<sup>37</sup> The magnesium oxidation number in the magnesium complex of core-modified porphyrin is desired here to be 0 for magnesium to act as an electron donor to silicon, and thus we use, as a substituent, the magnesium complex of

(33) Møller, C.; Plesset, M. S. *Phys. Rev.* **1934**, *46*, 618.

(34) Wiberg, K. B. *Tetrahedron* **1968**, *24*, 1083.

(35) Reed, A. E.; Curtiss, L. A.; Weinhold, F. *Chem. Rev.* **1988**, *88*, 899.

(36) (a) Zintl, E. *Angew. Chem.* **1939**, *52*, 1. (b) Schäfer, H.; Eisenmann, B.; Müller, W. *Angew. Chem., Int. Ed. Engl.* **1973**, *12*, 694.

(37) Latos-Grazynski, L. In *The Porphyrin Handbook*; Kadashi, K. M., Smith, K. M., Guillard, R., Eds.; Academic Press: New York, 2000; Vol. 2, pp 361-416, and references cited therein.

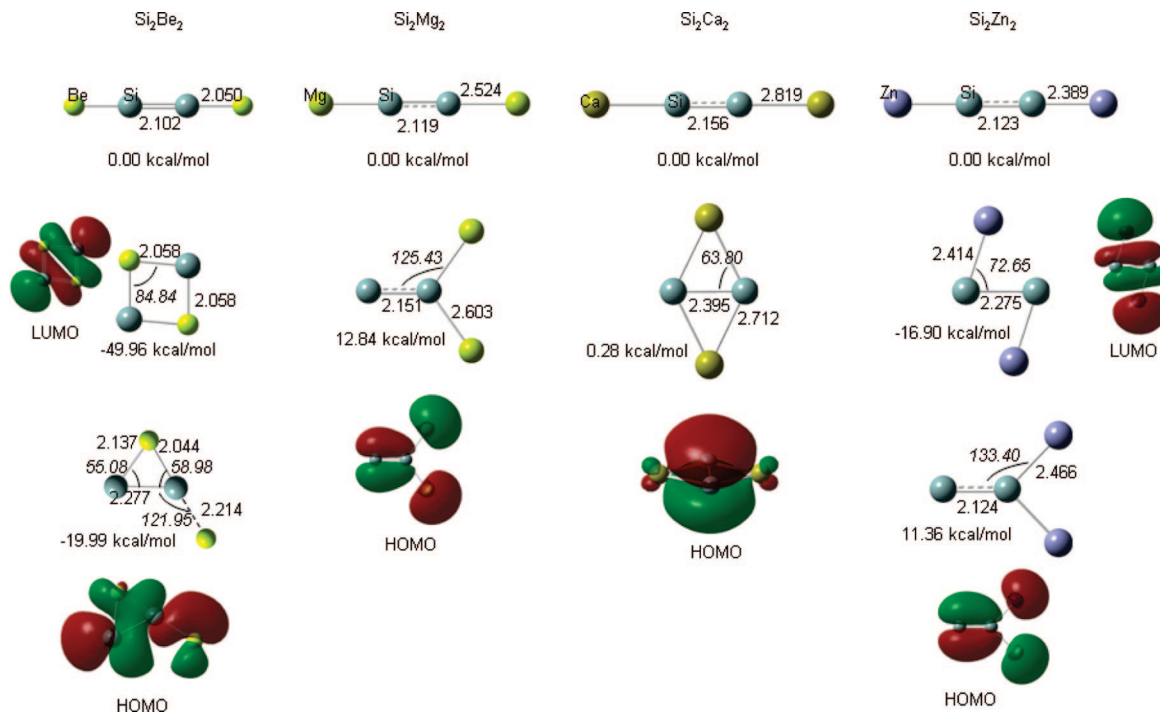


**Figure 3.** Optimized structures of  $E_2Si_2$  isomers at the MP2/6-311+G(3df) level and the molecular orbitals using the generalized density for MP2, where E = Be, Mg, Ca, Zn. Bond distances and bond angles (italics) are given in Å and deg, respectively. Energies relative to the corresponding linear isomer are given in kcal/mol with a ZPVE correction.

21,23-dioxaporphyrin, which was recently synthesized.<sup>38</sup> Due to the large molecular size, the calculation level is lowered for the geometry optimization of the disilyne with the magnesium complex of 21,23-dioxaporphyrin (**6**). It is confirmed that the MP2/3-21G level gives a minimum for a linear  $MgSi\equiv SiMg$  and a second-order saddle point for a linear  $HSi\equiv SiH$ , which is the same characterization of stationary points as that at a much higher level (MP2/6-311+G(3df)) in Table 1). However, on our computer system, the frequency calculation of **6** at the MP2/3-21G level was not completed in a reasonable CPU time. We decided to use B3LYP instead. We can accept the B3LYP/3-21G level here as an adequate alternative, because B3LYP also gives a minimum for a linear  $MgSi\equiv SiMg$  and a second-order saddle point for a linear  $HSi\equiv SiH$  using the 3-21G basis set. The optimized structure of **6** gives a linear  $Si\equiv Si$  structure as a minimum at the B3LYP/3-21G level. We have also carried out the optimization with a larger basis set (6-31+G(d)) for the linear form of compound **6** (Figure 4) and  $MgSi\equiv SiMg$  for comparison. Unfortunately, the linear form is not a minimum at the B3LYP/6-31+G(d) level, which is the same characterization as that at the much higher level of calculations using the B3LYP method in Table 1. It may not be clear at present whether the linear **6** is a minimum or a saddle point, but we anticipate that it would be a minimum at the MP2/6-311+G(3df) level. The optimized Si–Si bond distance (2.108 Å) of **6** at the B3LYP/6-31+G(d) level is slightly longer than that (2.092 Å) of  $MgSi\equiv SiMg$  but is shorter than the usual Si–Si double bond (2.14 Å). It is noted here that the charge transfer between the Si and Mg atoms is reproduced (NPA charges are  $-0.392$  at Si and  $1.243$  at Mg) in compound **6**.

In conclusion, it is found from the present theoretical studies that, among several metal-substituted disilynes, the Mg-

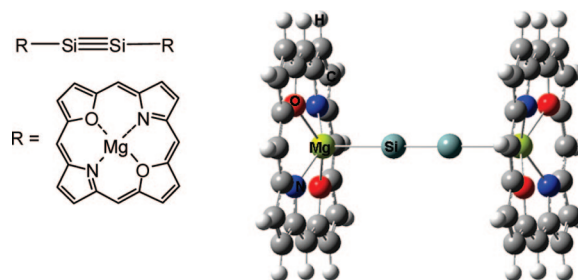


**Figure 4.** Optimized structure of **6** at the B3LYP/6-31+G(d) level. The Si–Si and Si–Mg bond lengths of  $MgSi\equiv SiMg$  are 2.092 and 2.639 Å, at the B3LYP/6-31+G(d) level, respectively.

substituted disilyne is highly suited to stabilize the linear conformation of the Si–Si triple bond. The Si–Si triple bond with  $D_{\infty h}$  symmetry beyond the multiple-bond rule is realized by the suppression of  $\sigma$ – $\pi$  mixing with the HOMO, which is neither a  $\sigma$  nor a  $\pi$  orbital. The linear  $MgSi\equiv SiMg$  gives a Wiberg bond index of 2.923 (much closer to 3 than trans-bent disilynes) and a short Si–Si bond length of 2.119 Å. The six valence electrons are accommodated in one  $\sigma$  and two degenerate  $\pi$  molecular orbitals, as in the case of a classical triple bond. From the survey of the isomeric potential energy surface,  $Mg_2Si_2$  has two isomers (linear and disilavinylidene) and the linear structure is more stable by approximately 10 kcal/mol. On the basis of the present theoretical studies, a synthetically accessible disilyne with the classical linear structure is designed using the magnesium complex of 21,23-dioxaporphyrin as a substituent.

**Supporting Information Available:** Tables of Cartesian coordinates of **6** optimized at the B3LYP/3-21G and B3LYP/6-31+G(d) levels. This material is available free of charge via the Internet at <http://pubs.acs.org>.

OM800469W

(38) Punidha, S.; Agarwal, N.; Burai, R.; Ravikanth, M. *Eur. J. Org. Chem.* **2004**, 10, 2223.